

**MCNP6.1 Computation of Fluence-to-Ambient Dose Equivalent Conversion Factors for a Steel Cube**S. R. McHale,<sup>a</sup> M. Millett,<sup>a</sup> A. W. Decker<sup>b</sup><sup>a</sup>United States Naval Academy, 590 Holloway Road, Annapolis, MD 21402, mchale@usna.edu; millett@usna.edu<sup>b</sup>Defense Threat Reduction Agency Nuclear Science and Engineering Research Center (DTRA-NT-NSERC), United States Military Academy Building 753, West Point, NY, 10996, Andrew.Decker@usma.edu**INTRODUCTION**

Over the last two decades, the ballistic shielding of U.S. military vehicles has evolved rapidly to meet dynamic global threats, but the degree of protection provided by these novel materials against the effects of ionizing radiation is not well measured or calculated. During the Cold War-era, the U.S. Army quantified—justifiably—the radiation protection factors of simplified, surrogate vehicles via experiments at pulsed radiation facilities and using discrete ordinates and Monte Carlo codes, specifically MCNP4 [1-3]. Although many of the test facilities no longer operate, computational capabilities have advanced to the extent that high-fidelity simulations of radiation transport and interactions through detailed vehicle geometries are attainable in reasonable run times. The robust, versatile features of the current MCNP6 code offer new, reliable, and cost-effective methods that can estimate the response of current equipment in the military inventory to the potentially harmful effects of nuclear radiation. Characterizing these responses has important consequences should the U.S. ever be confronted by a nuclear attack, but there are less hyperbolic scenarios where the detailed response functions would be valuable. For example, during the 2011 Operation Tomodachi disaster relief effort that followed the Tohoku, Japan earthquake and subsequent tsunami, radiation protection information was requested by, but unavailable to, operational decision-makers in the area of the damaged Fukushima Daiichi nuclear power plant [4]. With these considerations in mind, we are conducting ongoing experimental and computational studies of simple geometries and materials, as well as multi-layer, nonhomogeneous surrogate structures, in an effort to compute, validate, and measure the responses of various materials to both monoenergetic sources of nuclear radiation and spectra of neutrons and photons.

**METHODOLOGY****Overview**

The International Commission on Radiological Protection (ICRP) recommends the ambient dose equivalent  $H^*(10)$  as the appropriate operational quantity to assess the dose from radiation fields for the purpose of protection [5]. The quantity  $H^*(10)$  is defined as the dose equivalent produced at a depth of 10 mm in a 30-cm, tissue-equivalent sphere that is located at a point in the aligned and expanded

radiation field, where tissue-equivalent means unit density ( $1 \text{ g cm}^{-3}$ ) and mass composition of 76.2% oxygen, 11.1% carbon, 10.1% hydrogen, and 2.6% nitrogen [6]. The geometry and material composition of the tissue-equivalent sphere were defined in MCNP6.1 [7], and values for fluence-to-ambient dose equivalent conversion factors,  $H^*(10)/\phi$ , were computed for both photon and neutron radiation fields in absence of shielding (unshielded) and with the sphere enclosed by a 1-in thick cube of steel (shielded). The calculated values of  $H^*(10)/\phi$  for photons and neutrons in the unshielded geometry were compared to Tables A.21 (photons) and A.42 (neutrons) of ICRP 74 [8], in order to validate the computational method, while  $H^*(10)/\phi$  values in the shielded geometry can be applied to quantify the radiation protection of steel in the presence of monoenergetic sources of radiation as well as photon and neutron spectra.

All simulations were conducted using the analog Monte Carlo model, which replicates scattering, absorption and other events by sampling from tabulated cross sections that are distributed with the MCNP code. Computational uncertainty due to random error was minimized by increasing the number of simulated events until acceptable results with MCNP-reported relative errors less than 10% were obtained. We realize that this method will be impractical for more complex materials and geometries where few source particles will reach the regions where tallies are computed, and for those studies, non-analog simulations that apply variance reduction methods available in MCNP will be analyzed to determine the technique, or combination of methods, that minimizes computation time and sources of error. Finally, MCNP input data cards were generated to assure that interaction cross sections were sampled from the *endf71x* library, which is distributed with MCNP6.1 and based on recent, thoroughly-evaluated nuclear data files from ENDF/B-VII.1.

**Calculation of  $H^*(10)/\phi$  for Photons**

The gamma-ray radiation fields were simulated as uniformly-distributed, planar sources of monoenergetic photons (typically  $10^7$  gamma rays) at 25 energies from 10 keV to 10 MeV, which correspond to Table A.21 of ICRP 74. For each gamma-ray energy, the ambient dose equivalent was calculated by recording the MCNP f6 tally (absorbed dose) inside a 1-mm side cube that was centered at a depth of 10 mm from the edge of the 30-cm diameter tissue-equivalent sphere, as specified in the  $H^*(10)$  definition. The MCNP-computed absorbed doses from

photons, which have a radiation weighting factor of unity, were then used to calculate the fluence-to-ambient dose equivalent conversion factors via

$$\frac{H_{\gamma}^*(10)}{\phi} = 640.8 \text{ (f6 tally)} r^2 \left[ \frac{\text{pSv} \cdot \text{cm}^2}{\text{source part.}} \right], \quad (1)$$

where the constant 640.8 converts the f6 tally from units of MeV/g to those shown at the right of equation (1), and  $r$  is the radius of the tissue sphere.

Error bars were constructed for each simulation from the MCNP-computed relative standard error

$$R \equiv S_{\bar{x}} / \bar{x}, \quad (2)$$

where  $\bar{x}$  is an estimator of the mean—the f6 tally for these simulations—and  $S_{\bar{x}}$  estimates the standard error of the mean. Values of  $R$  were applied to form confidence intervals, where the true result of the computed tallies, and hence the fluence-to-dose conversion factors, are in the range  $\bar{x} (1 \pm R)$  with a likelihood of 68%, as stated by the Central Limit Theorem.

### Calculation of $H^*(10)/\phi$ for Neutrons

The neutron radiation fields were simulated as planar sources of monoenergetic neutrons (typically  $10^8$  particles) at 53 energies from  $10^{-9}$ –200 MeV, corresponding to Table A.42 of ICRP 74. To account for absorbed dose from both neutrons and neutron-induced photons, MODE N P was specified in the source definition (SDEF) of the data input card, and MCNP f6 tallies were recorded for the two interaction types. Conversion factors for neutron-induced photons,  $H_{(n,\gamma)}^*(10)/\phi$ , were determined as described by equation (1). For neutrons, these conversion factors were calculated from the absorbed doses by applying the energy-dependent ICRP 74 radiation weighting function [8]

$$w_n = 5 + 17 \text{Exp} \left[ \frac{-(\ln[2 E_n])^2}{6} \right], \quad (3)$$

where  $E_n$  is the energy of the neutron, in MeV, and the conversion factors were then computed as

$$\frac{H_n^*(10)}{\phi} = w_n 640.8 \text{ (f6 tally)} r^2 \left[ \frac{\text{pSv} \cdot \text{cm}^2}{\text{source part.}} \right]. \quad (4)$$

Finally, the total fluence-to-dose conversion factors from both neutrons and neutron-induced photons,

## Radiation Protection and Shielding: General

$H_{n+(n,\gamma)}^*(10)/\phi$ , were determined by adding the individual components.

Error bounds representing a 68% confidence interval on  $H_{n+(n,\gamma)}^*(10)/\phi$  were determined from MCNP-computed relative standard errors for the f6 tallies corresponding to absorbed doses from neutrons and neutron-induced photons, as well as the uncertainty of the neutron weighting factor from ICRP 74, which was assumed to be 10%. The appropriate uncertainties were then summed in quadrature to calculate confidence intervals and construct error bars.

## RESULTS

Figure 1 compares the MCNP6.1-computed and ICRP 74-published fluence-to- $H^*(10)$  conversion factors for an unshielded tissue-equivalent sphere within a photon radiation field. The calculated values agree well with the accepted published conversion factors.

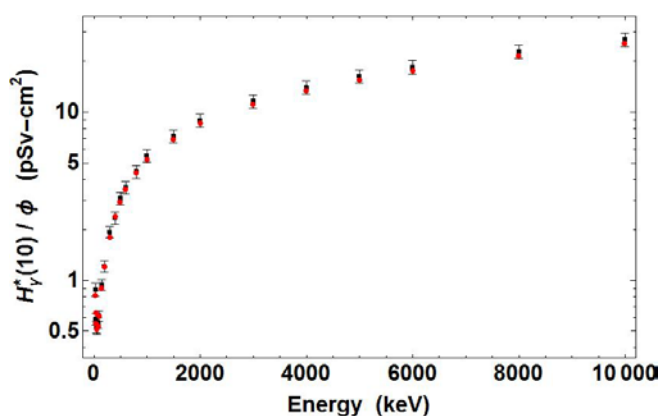


Fig. 1. Fluence-to-ambient dose equivalent conversion factors for an unshielded tissue-equivalent sphere within a photon radiation field, as computed by MCNP6.1 (black squares) and published in Table A.21 of ICRP 74 (red circles).

MCNP reports the results of ten statistical checks for each tally specified on an input card, and many of the 25 simulations shown in Figure 1 passed all tests, while all met the criteria for behavior of the tally mean and relative standard error. However, closer examination of output files for several photon energies showed that the number of histories was not sufficient to sample rare, high-scoring events that contribute to the absorbed dose; this observation is enumerated in MCNP as the slope of the empirical probability distribution function for the tally. While increasing the simulated histories might sample the uncommon events appropriately, we suspect that population control methods (e.g. weight windows, energy and geometry splitting/roulette) and other variance reduction techniques

available in MCNP will prove more efficient than increasing the histories. Similar observations were noted for the figures that results that follow and, as stated previously, future examinations will emphasize variance reduction methods.

Figure 2 compares the MCNP6.1-computed and ICRP 74-published fluence-to- $H^*(10)$  conversion factors for an unshielded, tissue-equivalent sphere within a neutron radiation field. For neutrons between 30 keV and 0.5 MeV, the calculated values agree well with the accepted published conversion factors. Below 30 keV, the values differ by a factor of 2–3, and above 0.5 MeV the disparity is approximately 1.5. Potential sources of discrepancies include the functional form of  $w_n$  and fidelity of MCNP neutron cross sections. Additional studies will be completed to assess the validity of the claims.

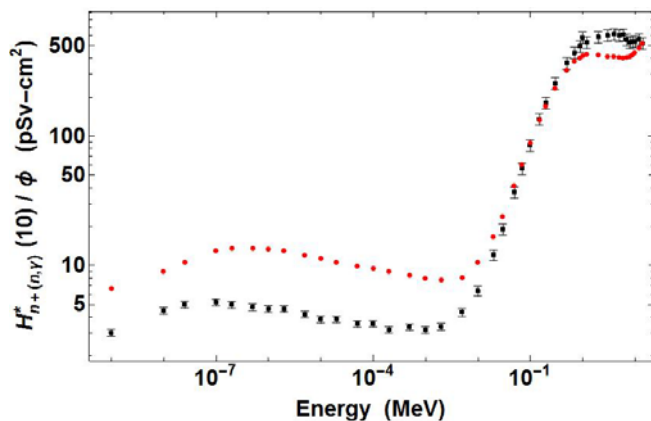


Fig. 2. Fluence-to-ambient dose equivalent conversion factors for an unshielded tissue-equivalent sphere within a neutron radiation field, as computed by MCNP6.1 (black squares) and published in Table A.42 of ICRP 74 (red circles).

Figure 3 shows the MCNP6.1-computed fluence-to- $H^*(10)$  conversion factors for a tissue-equivalent sphere that is unshielded from a photon radiation field, and the tissue sphere shielded within a 1-inch thick steel cube. The steel appears to be roughly equally effective at reducing the ambient dose equivalent across the range of photon energies; this statement needs to be quantified further.

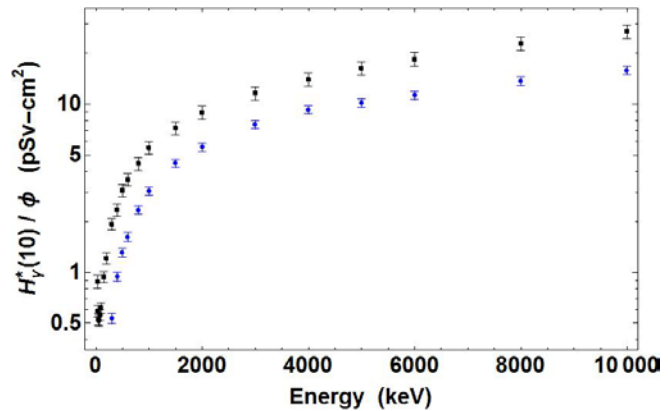


Fig. 3. MCNP 6.1-computed fluence-to-ambient dose equivalent conversion factors for an unshielded tissue-equivalent sphere in a photon radiation field (black squares) and the same tissue sphere shielded within a 1-in thick steel cube (blue squares).

Figure 4 compares the MCNP6.1-computed fluence-to- $H^*(10)$  conversion factors for a tissue-equivalent sphere that is unshielded from a neutron radiation field, and the tissue sphere shielded within a 1-inch thick steel cube. The comparison shows that  $H^*(10)$  in the shielded configuration exceeds the unshielded  $H^*(10)$  for neutron energies less than 10 keV, which indicates that the geometry and composition of the shield moderate the radiation field to neutron energies with interaction cross sections that exceed values in the unshielded geometry.

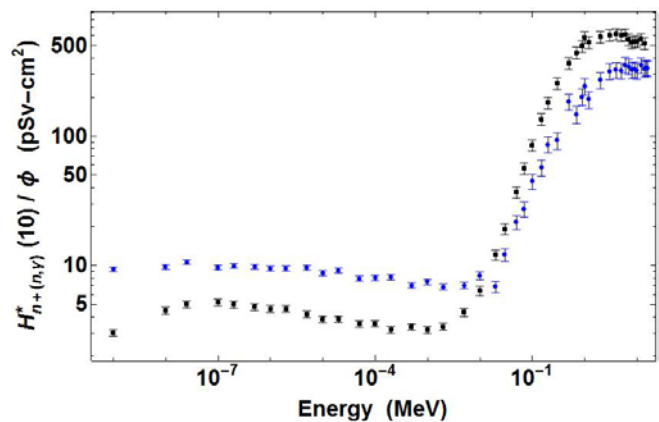


Fig. 4. MCNP 6.1-computed fluence-to-ambient dose equivalent conversion factors for an unshielded tissue-equivalent sphere in a neutron radiation field (black squares) and the same tissue sphere shielded within a 1-in thick steel cube (blue squares).

**REFERENCES**

1. C.R. Heimbach, "Radiation Protection-Factor Measurements of a Lined Iron Box in Simulated Fission and Fusion Tactical Nuclear Environments," Army Pulse Radiation Directorate, Aberdeen Proving Grounds, MD (1985).
2. C.R. Heimbach, "Final Report of Radiation Shielding in Armored Vehicles," Defense Technical Information Center, Alexandria (1988).
3. C. Eisenhauer and L. Spencer, "Approximate Procedure for Calculating Protection From Initial Nuclear Radiation From Weapons," National Bureau of Standards Center for Radiation Research, Gaithersburg (1988).
4. J.C. Nellis and J.F. Marquart, "Protection Factors of Combat Systems," *Combating WMD Journal*, **8**, 44-46 (2012).
5. International Commission on Radiological Protection, The 2007 Recommendations of the International Commission on Radiological Protection, ICRP Publication 103 (2007).
6. International Commission on Radiation Units and Measurements, Determination of Dose Equivalents Resulting from External Radiation Sources, ICRU Report 39 (1985).
7. "Initial MCNP6 Release Overview – MCNP6 Version 1.0," Los Alamos National Laboratory report LA-UR-13-22934 (2013).
8. International Commission on Radiological Protection, Conversion Coefficients for Use in Radiological Protection against External Radiation, ICRP Publication 74 (1996).